A thermo-magnetic bag model for the quark-gluon plasma

P. F. Valenzuela-Coronado[a], M. E. Tejeda-Yeomans[b], and J. Torres-Arenas[a]

[a]*División de Ciencias e Ingenierías, Campus León, Universidad de Guanajuato, México.*
e-mail: paulinafvc95@gmail.com; jtorres@fisica.ugto.mx
[b]*Facultad de Ciencias - CUICBAS, Universidad de Colima,*
Bernal Díaz del Castillo No. 340, Col. Villas San Sebastián, 28045 Colima, México.
e-mail: matejeda@ucol.mx

Received 1 August 2023; accepted 26 October 2023

In this work we study the pressure of the quark-gluon plasma in the presence of a magnetic field, using a minimally enhanced model of a weakly interacting gas of quasi-particles in a thermal bath. We include the magnetic field effects through the quark mass that has been modified using a recently proposed thermo-magnetic coupling. This thermo-magnetic coupling emerges form the quark-gluon vertex in the HTL approximation [1]. We use Lattice QCD [2] data, to constrain the thermo-magnetic bag function of the quasi-particle model and provide an estimate of the thermo-magnetic vacuum energy density. We then compute the transverse pressure of the system and compare with similar results from the literature. We find that this thermo-magnetic coupling allows a robust description of this Lattice QCD data for the pressure of the QGP in the presence of a magnetic field. The extension to the thermal quasi-particle model we have introduced here, makes it easier to pursue further phenomenological studies that require simulations with an EoS that has integrable quasi-particle thermodynamic variables which have the general features of lattice data in the weak magnetic field regime.

Keywords: Quark-gluon plasma; quasi-particles; thermo-magnetic;

DOI: https://doi.org/10.31349/RevMexFis.70.021201

1. Introduction

The quest to produce and characterize the quark-gluon plasma (QGP) in heavy-ion colliders, provides a real possibility to probe extreme phenomena occurring during the early stages of this fireball of strongly interacting fluid-like matter (for a review, see [3] and references therein). These experiments involve the acceleration and interaction of heavy-ions, which create the right conditions for intense magnetic fields to be produced not only by the spectator nuclei, but also by the swirly QGP created in the overlapping region [4-12]. These dynamic magnetic fields may impact the QGP evolution at different stages and they may lead to spin alignment and polarization [13-16], magnetic catalysis and inverse magnetic catalysis, chiral magnetic effect and charge segregation, and many other interesting phenomena [2,17-21]. In the heavy-ion community there are diverse efforts in the development of experimental protocols and phenomenological studies to find signatures of these magnetic fields in the usual and new observables [22-26].

One of the crucial tools to learn about the behaviour of strongly-interacting quarks and gluons under extreme conditions of temperature and external magnetic fields, is to study Quantum Chromodynamics (QCD) in a constant background magnetic field using lattice simulations [2,27-30]. This framework provides an in-depth quantitative knowledge of the QCD equation of state (EoS). It connects the high temperature phase with quarks as relevant degrees of freedom, with the low temperature phase where light hadrons dominate the dynamics. Thus the EoS encodes the effects of the external magnetic field in the so called magnetic susceptibility of the medium. Recently, the magnetic susceptibility of thermal QCD matter using lattice simulations was obtained and reported in Ref. [2]. There, the authors found diamagnetic behavior (negative susceptibility) at low temperatures and strong paramagnetism (positive susceptibility) at high temperatures, which was reported with a quite simple parametrization of the temperature- and magnetic field-dependence of thermodynamic properties. This has allowed us to report here an extended phenomenological model, a thermo-magnetic quasi-particle model to study the longitudinal and transverse pressure of the QGP-like system.

Together with the lattice approach, there are field theoretical treatments of QGP-like systems involving quarks and gluons at finite temperature and in the presence of magnetic fields. In the literature, the study of QGP-like systems using large values of the temperature and/or the magnetic field, has been reported using a wide variety of frameworks: perturbation theory, chiral perturbation theory, the Hard Thermal Loop (HTL) approximation and effective models [31-43]. In particular, there is an approach that naturally includes the plasma screening effects [44] that arise in these kind of extreme conditions. In fact, as part of the HTL efforts, in Ref. [1] the HTL approximation was implemented to get the leading behavior of the QCD coupling for weak magnetic fields at high temperature, where the fermion mass acts as the infrared regulator. In their calculation, the thermo-magnetic dependence of the QCD coupling is extracted from the quark-gluon vertex in the weak field approximation. Under this approximation, the magnetic field strength is smaller than the square of the temperature, but it does not imply a hierarchy with respect to other scales in the problem such as the fermion mass.

In this work we use a quasi-particle picture to study the thermodynamical properties of the QGP in the presence of a magnetic field by including these effects through an effective mass for the quarks. The key ingredient to get this effective mass is the thermo-magnetic coupling reported in Ref. [1]. Then we use Lattice QCD data [2] to constrain the thermo-magnetic *bag function*, to be able to study the longitudinal and transverse pressure of the system. We then compare to similar results in the literature and we comment on the consequences of the proposed thermo-magnetic coupling used here.

The work is organized as follows: In Sec. 2 we review a successful quasi-particle model that includes confinement and in Sec. 3 we perform a minimal extension to this model so that it now includes thermo-magnetic effects. In Sec. 4 we compare the pressure from the thermo-magnetic quasi-particle model with recent Lattice QCD in a magnetic field data and extract a thermo-magnetic bag function. We then use the newly build thermo-magnetic pressure that includes a bag function, to report on the corresponding longitudinal and transverse pressure. Finally in Sec. 5 we summarize our results and comment on future avenues to pursue using this thermo-magnetic quasi-particle model.

2. Review of a self-consistent thermal quasi-particle bag model

In their seminal work R.A. Schneider and W. Weise [31] developed a framework which allows for a quasi-particle description of QCD thermodynamics. They built a successful quasi-particle interpretation of QCD EoS at finite temperature for the deconfined phase, using thermal masses and a phenomenological parametrization of the onset of confinement, in the vicinity of the predicted phase transition. One way to understand the thermal excitations arising in the QGP as a result of the strong interactions between quarks and gluons, implies a departure from ideality in model-building. From a quantum point of view, these excitations are called quasi-particles and play a similar role in the QGP than phonons in a solid. This allows for a model description of the QGP as a gas of quasi-particles with effective masses which depend on thermodynamic variables and the magnetic field [31,45-49].

In order to study the thermodynamic properties of the QGP in the presence of a magnetic field, we will include the relevant features of both confinement and thermo-magnetic effects on the mass and strong coupling into the framework of Ref. [31], which allows for a quasi-particle description of lattice QCD thermodynamics. In Ref. [31] the starting point is the pressure, which is an account of the free energy of a large volume and homogeneous system, which is obtained via the partition function for an ideal gas of relativistic quasi-particle fermions and bosons $p/T = \partial \ln Z/\partial V$ and can be written as

$$p(T) = \frac{\nu_g}{6\pi^2}\int_0^\infty \mathrm{d}k\; C(T)\; f_B(E_k^g)\; \frac{k^4}{E_k^g} + \frac{2N_c}{3\pi^2}\sum_{q=1}^{N_f}\int_0^\infty \mathrm{d}k\; C(T)\; f_D(E_k^q)\frac{k^4}{E_k^q} - B(T), \quad (1)$$

where $\nu_g = 2(N_c^2-1)$ is the gluon degeneracy factor, N_c the number of colors, N_f the number of flavors and the Fermi-Dirac and Bose-Einstein distributions at zero chemical potential are $f_D(E) = (\exp(E/T)+1)^{-1}$ and $f_B(E) = (\exp(E/T)-1)^{-1}$, respectively. The thermal effects are also included in the single particle energy for quarks and gluons, given as

$$E_k^{q,g} = \sqrt{k^2 + m_{q,g}^2(T)}\,, \quad (2)$$

where $m_{g,q}(T)$ are the quark and gluon effective masses generated dynamically by their interaction in a heat bath at temperature T. The thermal masses are obtained from the self-energies of the corresponding particles, evaluated at thermal momenta $k \sim T$ as

$$m_q^2(T) = m_{0q}^2 + C_F\,\frac{T^2}{4}G^2(T), \quad (3)$$

$$m_g^2(T) = \left(C_A + \frac{N_f}{2}\right)\,\frac{T^2}{6}G^2(T), \quad (4)$$

where the Casimir color factors for the fundamental and adjoint representations are $C_F = (N_c^2-1)/2N_c$ and $C_A = N_c$, respectively, and m_{0q} is the zero-temperature bare quark mass. The dimensionless effective coupling $G(T)$ includes a pseudo-critical behavior when the heat bath temperature T approximates a critical temperature T_c

$$G^2(T) = \frac{g_0^2}{11N_c - 2N_f}\left([1+\delta] - \frac{T_c}{T}\right)^{2\beta}. \quad (5)$$

The constant g_0 and the characteristic exponent β are chosen so that asymptotically $G(T)$ makes the thermal masses in Eqs. (3) and (4) match those of the Hard Thermal Loop (HTL) perturbative form, when $T \gg T_c$ and are extracted from fits to Lattice QCD data [27–30]. Note also that the thermal masses have a functional critical behaviour, $m_{q,g}(T) \approx (T-T_c)^\beta$, around T_c.

Furthermore, this quasi-particle model of the QGP at finite temperature, proposes that the general thermodynamic features of this strongly interacting plasma, can be described in terms of effective degrees of freedom that include a statistical parametrization of confinement through

$$C(T, \mu = 0) = C_0\left([1+\delta_c] - \frac{T_c}{T}\right)^{\beta_c}, \quad (6)$$

where the parameters C_0, δ_c and β_c are also extracted with fits to Lattice QCD data [27–30]. This implementation of confinement in a statistical system, provides a numerical strategy to include effects due to the number of thermally active gluons as a function of temperature. This implementation

is certainly not unique, since confinement could emerge directly from an effective coupling. The model we will present in the next section provides a platform to implement more sophisticated confiment models. This is work in progress, and it will be reported elsewhere.

In the work we report here, we will extend this model and we will test our results using $N_c = 3$ and $N_f = 2$ and the parameter fit corresponding to *Set B*, as reported in Table I of Ref. [31]: $g_0 = 9.4$, $\beta = 0.1$ and $\delta = 10^{-6}$. For the parametrization of confinement, we will use $C_0 = 1.03, \delta_c = 0.02, \beta_c = 0.2$. Also, in the rest of this work we will use the pion mass $m_\pi = 0.139$ GeV as the proxy scale to explore the dynamics for $T_c \sim m_\pi$.

In this thermal quasi-particle model, the thermodynamic consistency is achieved in the way the energy and entropy densities are built together with Eq. (1). First note that, the pressure in Eq. (1) has been modified by subtracting $B(T)$, a *bag function*. This function acts as a background field, and it is a negative (positive) contribution to the pressure (energy density) inside *the bag*, thus creating a confining mechanism that is not emerging dynamically, but rather is put in by hand. Also, as we will see in a moment, it helps maintain thermodynamic consistency since the quark and gluon thermal masses in Eqs. (3) and (4) have non-trivial dependence on the temperature.

A tool to monitor the thermodynamic consistency for a system at finite temperature and chemical potential is the Gibbs-Duhem relation in which the particle number N, entropy S and volume V of the system, are related through changes in their corresponding conjugate variables $N\ d\mu = -S\ dT + V\ dP$. In this work we focus on systems with zero chemical potential so the Gibbs-Duhem relation simplifies and the entropy density is directly connected to changes in the pressure with respect to temperature as follows

$$s \equiv \frac{S}{V} = \left.\frac{\partial p}{\partial T}\right|_{\mu} . \tag{7}$$

Furthermore, to ensure homogeneity of the thermodynamic potential, the Euler relation for zero chemical potential $U = TS - pV$ is used. In terms of the energy density ϵ and the entropy density s, this relation is given by

$$\epsilon + p = T\ s\ . \tag{8}$$

The combined Gibbs-Duhem and Euler relations given by Eq. (7) and Eq. (8), have been used as a thermodynamic criterion that must be satisfied in the context of statistical systems. A suitable and general discussion about this point can be found in Ref. [50]. Eq. (1) for the pressure, together with the energy and entropy densities as

$$\begin{aligned} s(T) &= \frac{\nu_g}{2\pi^2 T}\int_0^\infty \mathrm{d}k C(T) f_B(E_k^g)\left[\frac{4}{3}k^2 + m_g^2(T)\right]\frac{k^2}{E_k^g} \\ &\quad + \frac{2N_c}{\pi^2 T}\sum_{q=1}^{N_f}\int_0^\infty \mathrm{d}k C(T) f_D(E_k^q)\left[\frac{4}{3}k^2 + m_q^2(T)\right]\frac{k^2}{E_k^q}, \\ \epsilon(T) &= \frac{\nu_g}{2\pi^2}\int_0^\infty \mathrm{d}k\ C(T)\ f_B(E_k^g)\ k^2\ E_k^g \\ &\quad + \frac{2N_c}{\pi^2}\sum_{q=1}^{N_f}\int_0^\infty \mathrm{d}k\ C(T)\ f_D(E_k^q)\ k^2\ E_k^q + B(T), \end{aligned} \tag{9}$$

provide a complete thermodynamic description of the system. In Eq. (1) the bag term $B(T)$ acts as a negative pressure, but in Eq. (9) it adds to the energy density of the quasi-particles, so it can be interpreted as the thermal energy density of the Yang-Mills vacuum. One of the popular features of this model EoS is that it has no free fit parameters once the non-perturbative thermal behaviour of the quark and gluon masses are fixed. The confinement factor $C(T)$ in Eq. (6) then emerges from the ratio of the entropy density of Lattice QCD and the entropy density calculated with the thermal masses. In this way, $B(T)$ is fixed through the Gibbs-Duhem condition and we can recover the HTL results when $C(T) \to 1$, beyond the critical temperature.

3. A quasi-particle bag model with a thermo-magnetic coupling

In heavy-ion collisions the formation of intense magnetic fields with a short lifetime is possible and several observables are being proposed and studied in order to have access to measure the impact of these fields in the evolution of the QGP. If the intense magnetic fields are short lived then it is possible to have modifications in the propagation of quarks and gluons in the heat bath at temperature T, due to a *weak* magnetic field where $q\mathcal{B} \lesssim T^2$. In Ref. [1] the authors calculated the thermo-magnetic correction to the quark-gluon vertex in the presence of a weak magnetic field within the HTL approximation and from that, they extracted the effective thermo-magnetic quark-gluon coupling. They showed that this coupling decreases as a function of the magnetic field strength which is a useful feature to understand the inverse magnetic catalysis phenomenon.

In the work we report here, we want to minimally modify the purely thermal quasi-particle model we reviewed in Sec. 2 to be able to include the effects of a magnetic field in the development of longitudinal and transverse pressure of a QGP system. Taking advantage of the results of Ref. [1], the minimal step to this is to include the magnetic field effects through the quark effective mass. This in turn, can be done directly using a new dimensionless coupling based on

the thermo-magnetic coupling reported in Ref. [1]. Recent data from Lattice QCD in the presence of magnetic fields [2] can be then used to constrain the thermo-magnetic bag function which allows for the extraction of the longitudinal and transverse prassure of the QGP system.

Let us then focus on the thermo-magnetic pressure of the QGP in the presence of a magnetic field, where instead of Eq. (1) we now have

$$p(T,\mathcal{B}) = \frac{\nu_g}{6\pi^2}\int_0^\infty \mathrm{d}k\; C(T)\; f_B(E_k^g)\;\frac{k^4}{E_k^g} + \frac{2N_c}{3\pi^2}\sum_{q=1}^{N_f}\int_0^\infty \mathrm{d}k\; C(T)\; f_D(E_k^q)\;\frac{k^4}{E_k^q}, \qquad (10)$$

where the magnetic field dependence enters through the single particle energy for quarks only, and is given by

$$E_k^q = \sqrt{k^2 + m_q^2(T,\mathcal{B})}. \qquad (11)$$

Even though the gluon thermal mass in Eq. (4), could also receive magnetic corrections through fermion loops, for this minimally modified quasi-particle model, we will keep the gluon mass with only the thermal correction. In this minimal extension to the thermal quasi-particle model, the quarks carry an effective thermo-magnetic mass given by

$$m_q^2(T,\mathcal{B}) = m_q^2(T) + C_F\;\frac{T^2}{4}\mathcal{G}_q^2(T,\mathcal{B}), \qquad (12)$$

where we now propose and use the following dimensionless coupling

$$\mathcal{G}_q^2(T,\mathcal{B}) = \frac{g_0^2}{32\pi}\frac{|q\mathcal{B}|}{T^2}\left(\frac{2\ln(2)}{\pi} - \frac{T}{m_q(T)}\right)^{2\beta}, \qquad (13)$$

which includes the characteristic exponent β and the parameters as defined for the purely thermal coupling given by Eq. (5). As we will see in the next section, an advantage of this minimal extension to the thermal quasi-particle model is that we can add a bag function $B(T,\mathcal{B})$ to Eq. (10) if needed. Eqs.(11)-(13), represent an effective way to include the linear terms in the magnetic field otherwise expected from an actual treatment of the Landau level resummation (see for example [51] and references therein). A comprehensive analysis of all the limiting cases and approximations using models needed to arrive to the best thermo-magnetic masses and couplings is part of ongoing efforts of the theoretical heavy-ion physics community and are key to advance our understanding of the EoS of nuclear matter. The inclusion of thermo-magnetic effects on the description of the QGP produced in heavy-ion collisions has been widely discussed in the literature [52-56], including now different analysis on transport effects and baryon production [57]. The coupling we propose here in Eq. (13) is based on the thermo-magnetic effective coupling $g_{\rm eff}$ in Eq. (59) of Ref. [**?**] corresponding to a phenomenological situation in which a pair quark-anti-quark travel through a medium at temperature T in the presence of a weak magnetic field $\mathcal{B}$. The calculation was done using the HTL approximation as a thermo-magnetic correction to the quark-gluon vertex in the presence of a weak magnetic field, and from there the effective thermo-magnetic coupling is given by

$$\frac{g_{\rm eff}}{g_0} = 1 - \frac{m_q^2(T)}{T^2} + \left(\frac{8}{3T^2}\right) g^2 C_F M^2(T, m_q(T), q\mathcal{B}), \qquad (14)$$

where

$$M^2(T, m_q(T), q\mathcal{B}) = \frac{q\mathcal{B}}{16\pi^2}\left[\ln(2) - \frac{\pi}{2}\frac{T}{m_q(T)}\right]. \qquad (15)$$

For this particular situation, the authors of Ref. [1] show that the effective thermo-magnetic coupling $g_{\rm eff}$ decreases as a function of the magnetic field and this decrease is more significant for larger values of the strong coupling α_s. In fact for $\alpha_s = 0.2 - 0.3$, $g_{\rm eff}$ decreases down to about 15-25% for the largest strength of the magnetic field within the weak field limit, when compared with the purely thermal coupling.

Now, the proposed modification of the quark mass comes from a calculation in which HTL was used and the dominant terms in an $q\mathcal{B}$ expansion were kept which matches the corresponding Lattice QCD data we will use, which also keeps the leading contribution of magnetic field in the magnetic suceptibilities. This does not mean that the domain of aplicability of our results for the thermodynamical properties is restricted in this range. It means that we include the dominant effects of the magnetic field when the temperature is the dominant scale of the problem.

In this work, we take advantage of this thermo-magnetic coupling to posit that implementing it as an effective thermo-magnetic mass for the quarks, allows a robust description of the Lattice QCD data for thermodynamic properties of the QGP in the presence of a magnetic field as reported in Ref. [2]. As we will show in the next section, we find that with this approach we achieve an all around good description of the pressure of the QGP under a magnetic field, which makes it easier to pursue further phenomenological studies that require simulations with and EoS and integrable quasi-particle thermodynamic variables that contain the general features of lattice data.

4. The pressure and bag function of the QGP in a magnetic field from the thermo-magnetic quasi-particle model

In this section we report on the implementation of the minimally modified thermal quasi-particle model as described in Sec. 3, to obtain the pressure of the QGP and to compare with Lattice QCD results that include magnetic field effects.

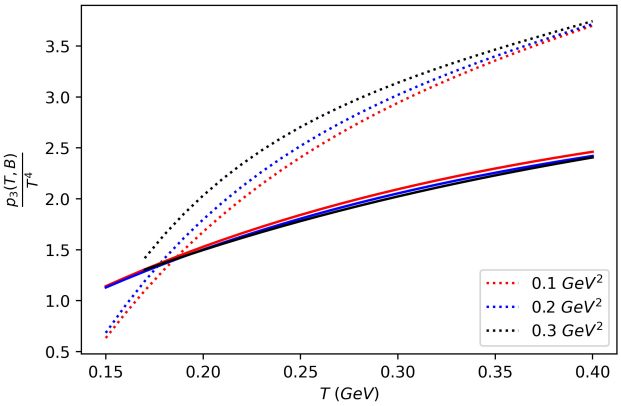

FIGURE 1. Pressure $p(T,\mathcal{B})$ scaled by T^4, for different values of the magnetic field $|q\mathcal{B}| = 0.1, 0.2, 0.3$ GeV^2 as a function of temperature T. Continous lines show the pressure from the quasi-particle thermo-magnetic model in Eq.(10) and dotted lines show the longitudinal pressure from Ref. [2] where they use a Lattice approach.

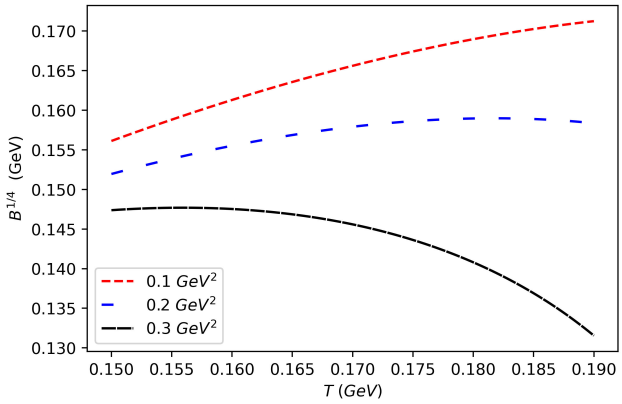

FIGURE 2. Effective bag function $B^{1/4}(T,\mathcal{B})$ extracted with Eq. (17) as a function of temperature T, for different values of the magnetic field $|q\mathcal{B}| = 0.1, 0.2, 0.3$ GeV^2. For $|q\mathcal{B}| = 0.1, 0.2$ GeV^2 the vacuum energy density from our model are within the range of those reported in the literature. For $|q\mathcal{B}| \geq 0.3$ GeV^2 and $T > 160$ MeV, the vacuum energy-density changes slope and tends to diminish. This indicates that the minimally modified thermo-magnetic quasi-particle model, requires less negative pressure from the bag in this regime, the magnetic field helps to maintain the pressure of the system.

In Fig. 1, the solid lines correspond to the temperature dependence of the pressure given by the minimally modified quasi-particle thermo-magnetic model in Eq. (10) normalized as p/T^4, for three values of the magnetic field $|q\mathcal{B}| = 0.1, 0.2, 0.3$ GeV^2. The same values of magnetic field are used to produce the dotted lines, which is the pressure normalized as p/T^4, given by the Lattice QCD. We use the results reported in Appendix F of Ref. [2] as a parametrization of the QCD EoS in a Python script `param_EoS.py` provided by the authors as an ancillary file to their arXiv manuscript. In this figure, we can see that pressure increases as the magnetic field increases, for both the model and the Lattice results. Nevertheless, the pressure given by Eq. (10) shows less sensitivity to the magnetic field effects as those reported in Ref. [2], and underestimates the pressure values, except for temperatures close to the critical temperature. The slope discrepancy between Lattice results and the minimally modified quasi-particle thermo-magnetic model can be a source of future enhancements to the model, since in general the change of p/T^4 with temperature (keeping constant the chemical potential) is

$$\frac{\partial}{\partial T}\left.\frac{p}{T^4}\right|_{\mu} = \frac{s}{T^4} - \frac{4}{T}\left(\frac{p}{T^4}\right). \tag{16}$$

In this sense, an underestimation of the slope in the quasi-particle model with respect to the Lattice results, indicates an underestimation of the QGP entropy density.

In order to improve the previous results we add a thermo-magnetic bag function $B(T,\mathcal{B})$ to Eq. (10), just as was done in the original thermal quasi-particle model in Eq. (1), as a negative pressure. We can then perform a numerical extraction of $B(T,\mathcal{B})$ for fixed values of the temperature and magnetic field, using the Lattice QCD results of Ref. [2], as

$$B(T,\mathcal{B}) = p(T,\mathcal{B}) - p^{\rm Latt}(T,\mathcal{B}), \tag{17}$$

where the leading-order expansion of the pressure in the magnetic field is given in terms of $\chi(T)$, the magnetic susceptibility

$$p^{\rm Latt}(T,\mathcal{B}) = p^{\rm Latt}(T,0) + \frac{\chi(T)}{2}(q\mathcal{B})^2. \tag{18}$$

Using this procedure, in Fig. 2 we plot the thermo-magnetic bag function as an estimation of the vacuum energy density $B^{1/4}(T,\mathcal{B})$ for $|q\mathcal{B}| = 0.1, 0.2, 0.3$ GeV^2. We can see that for the lower values of magnetic field, the vacuum energy density from our model is within the range of those reported in the literature (see for example [58, 59] and references therein). However, for larger values of the magnetic field and higher temperatures, the vacuum energy-density changes slope and tends to diminish. This indicates that the minimally modified quasi-particle model, requires less negative pressure from the bag in this regime.

Even though the system excitation is driven by the temperature in this regime and requires more negative pressure from the bag, this is less so when the magnetic field increases. This points to a regime in our model, where the magnetic field helps to maintain the pressure of the system. In order to validate the numerical implementation of Eq. (10) that now includes a thermo-magnetic bag function, Fig. 3 shows the temperature dependence of pressure (scaled with T^4) for magnetic field values $|q\mathcal{B}| = 0.1, 0.2, 0.3$. As expected -and by construction- the results from our model reproduces those of Lattice QCD [2] shown in Fig. 1. Now the model reflects interesting properties that were already there for the Lattice results. For example, note how the slopes of p/T^4 are greater for lower temperatures (closer to the critical temperature) and decrease for higher ones. According to Eq. (16), this implies that the thermodynamic relation $\epsilon > 3p$ or equivalently

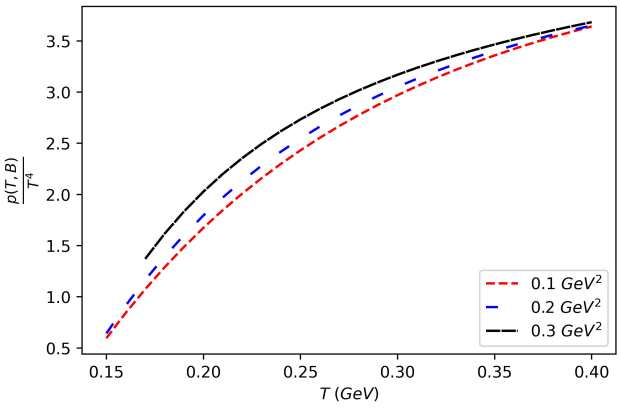

FIGURE 3. Pressure $p(T,\mathcal{B})$ scaled by T^4, for different values of the magnetic field $|q\mathcal{B}| = 0.1, 0.2, 0.3$ GeV^2 as a function of temperature T given by Eq. (10) which now includes a bag function $B(T,\mathcal{B})$ obtained as Eq. (17). As expected -and by construction- now the model reproduces the Lattice QCD results [2] shown in Fig. 1.

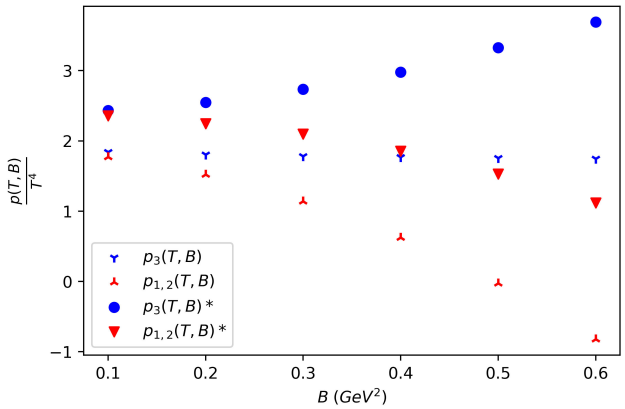

FIGURE 4. Longitudinal $p_3^*(T,\mathcal{B})$ and transverse $p_{1,2}^*(T,\mathcal{B})$ pressure scaled by T^4 calculated with the thermo-magnetic quasi-particle model that includes a bag function shown in Fig. 3 at a fixed $T = 250$ MeV, for different values of the magnetic field $|q\mathcal{B}| = 0.1 - 0.6$ GeV^2. Blue and red symbols represent longitudinal and transversal pressure, respectively. For comparison, we show the longitudinal $p_3(T,\mathcal{B})$ and transverse $p_{1,2}(T,\mathcal{B})$ pressure scaled by T^4 calculated with the thermo-magnetic quasi-particle model without a bag function shown in Fig. 1. The pressure range predicted from the model is approximately, 4×10^{-3} GeV $< p^* < 1.4 \times 10^{-2}$ GeV. Similar results have been reported in the literature with other methods, such as Ref. [60].

$TS > 4pV$, must be satisfied. So in this regime, the entropic forces are the ones driving the process rather than energetic ones.

It is known (see Ref. [30] and references therein) that in the presence of a background magnetic field, the different components of the pressure might become anisotropic. It is usual to distinguish between two schemes. In one of them, the flux of the magnetic field is kept constant (Φ-scheme); in the other one, it is the magnetic field strength which is fixed ($\mathcal{B}$-scheme). Up to now, we have been working under the $\mathcal{B}$-scheme, where the pressure is isotropic. However, in the Φ-scheme this is no longer true, the longitudinal pressure is scheme-independent but the transverse one is not. In the Φ-scheme, the transverse $p_{1,2}$ and longitudinal p_3 pressure components are related as

$$p_{1,2} = p_3 - q\mathcal{B} \cdot M, \tag{19}$$

where the magnetization can be written as the partial derivative of the free energy with respect to the magnetic field $M = -\partial f/\partial(q\mathcal{B})$ and it was also reported in Ref. [2]. Now, up to leading-order in the magnetic field, the magnetization is a linear function of $\mathcal{B}$. Therefore, the difference between longitudinal and transverse pressures is a quadratic function of the magnetic field (multiplied by a temperature function). We verify this, with the extraction of the longitudinal and transverse pressures with our thermo-magnetic model that now has a bag function to reproduce Lattice QCD results, but also we extract them with the original model without the bag function.

In Fig. 4, the longitudinal and transverse pressures at a fixed temperature $T = 250$ MeV, are presented. The longitudinal $p_3^*(T,\mathcal{B})$ and transverse $p_{1,2}^*(T,\mathcal{B})$ pressure scaled by T^4 calculated with the thermo-magnetic quasi-particle model that includes a bag function are shown in closed circles and triangles, whereas the ones from the original model without the bag function are $p_3(T,\mathcal{B})$ and $p_{1,2}(T,\mathcal{B})$. In this figure we can appreciate that with the proposed thermo-magnetic model without a bag function, we get a flat behavior of the longitudinal pressure for a range of magnetic field as expected from Fig. 1. Nevertheless the model on its own, has a benchmark description of the system that is not far from what is expected from Lattice. Once we use the thermo-magnetic model that includes the bag function, we recover what we expect from Lattice QCD. From the figure it follows that the pressure range predicted from the model is approximately, 4×10^{-3} GeV $< p < 1.4 \times 10^{-2}$ GeV. Similar results have been reported in the literature with other methods, such as Ref. [60].

5. Summary and outlook

In this work a quasi-particle bag model with a thermo-magnetic coupling was used in order to study the pressure of the QGP in the presence of a magnetic field. The QGP is modeled as a weakly interacting gas of quasi-particles whose masses incorporate the thermal and magnetic effects through an effective QCD coupling which we propose here in Eq. (13).

The quasi-particle thermo-magnetic model includes thermo-magnetic bag function Eq. (17), which we extract from recent Lattice QCD results [2], $B^{1/4}(T,\mathcal{B}) \sim 147 - 155$ MeV for $T \sim 150$ GeV and $B^{1/4}(T,\mathcal{B}) \sim 130 - 170$ MeV for $T \sim 190$ GeV gives an estimate for the thermo-magnetic vacuum energy density. The lower values for this vacuum energy density $B^{1/4}(T,\mathcal{B})$ were found for higher values of the magnetic field. This hierarchy points to a regime in our model, where the magnetic field effects included in the

quark effective mass through the thermo-magnetic coupling, are contributing to the pressure in such a way as to need a smaller bag function.

Once the bag function is included, the pressure in the $\mathcal{B}$-scheme is calculated for different values of the magnetic field, and a positive slope is found for the range of temperatures and magnetic fields considered. This result implies the dominance of the entropic term over the mechanical one, $TS > 4pV$, possibly indicating the prevalence of an entropic driven process instead an energetic driven one. In the Φ-scheme the results obtained for the transversal and longitudinal pressures show an increasing (decreasing) longitudinal (transversal) pressure as a function of the strength of the magnetic field.

Finally, the minimally extended quasi-particle model reported here allows a robust description of the Lattice QCD data for thermodynamic properties of the QGP in the presence of a magnetic field. The coupling that inspired the effective quark mass we are using in this model was obtained in Ref. [1] in a calculation in which HTL was used and only the leading terms in the magnetic field were kept during the analysis. As we use this as an input in our thermo-magnetic quasi-particle model, the domain of applicability of this model is not *a priori* restricted in this range. Further developments associated with improvements of this model will be reported elsewhere.

We find that with this approach, we achieve an all around good description of the pressure of the QGP under a magnetic field. This makes it easier to pursue further phenomenological studies that require simulations with an EoS that has integrable quasi-particle thermodynamic variables with the general features of Lattice QCD data.

Acknowledgments

This work was supported in part by Consejo Nacional de Humanidades, Ciencia y Tecnología grant numbers A1-S-7655 and CF-2023-G-433. M.E.T-Y. acknowledges support by the Simons Foundation through the Simons Foundation Emmy Noether Fellows Program at Perimeter Institute and is grateful for the hospitality of Perimeter Institute where part of this work was carried out. J.T.A. acknowledges support by Universidad de Guanajuato Grant No. 174/2023 of Convocatoria Institucional de Investigación Científica 2023.

1. A. Ayala, J. J. Cobos-Martínez, M. Loewe, M. E. Tejeda-Yeomans, and R. Zamora, *Phys. Rev. D* **91** (2015) 016007.
2. G. S. Bali, G. Endrõdi, and S. Piemonte, *JHEP* **07** (2020) 183.
3. M. E. Tejeda-Yeomans, *CERN Yellow Rep. School Proc.* **2** (2021) 137.
4. D. E. Kharzeev, L. D. McLerran, and H. J. Warringa, *Nucl. Phys. A* **803** (2008) 227.
5. V. Skokov, A. Y. Illarionov, and V. Toneev, *Int. J. Mod. Phys. A* **24** (2009) 5925.
6. V. Voronyuk *et al.*, *Phys. Rev. C* **83** (2011) 054911.
7. A. Bzdak and V. Skokov, *Phys. Lett. B* **710** (2012) 171.
8. W.-T. Deng and X.-G. Huang, *Phys. Rev. C* **85** (2012) 044907.
9. L. McLerran and V. Skokov, *Nucl. Phys. A* **929** (2014) 184.
10. G. Inghirami, M. Mace, Y. Hirono, L. Del Zanna, D. E. Kharzeev, and M. Bleicher, *Eur. Phys. J. C* **80** (2020) 293.
11. L. Oliva, *Eur. Phys. J. A* **56** (2020) 255.
12. K. Hattori, M. Hongo, and X.-G. Huang, *Symmetry* **14** (2022) 1851.
13. F. Becattini and M. A. Lisa, *Ann. Rev. Nucl. Part. Sci.* **70** (2020) 395.
14. A. Ayala, I. Domínguez, I. Maldonado, and M. E. Tejeda-Yeomans, *Phys. Rev. C* **105** (2022) 034907.
15. T. Niida, *EPJ Web Conf.* **271** (2022) 08008.
16. X.-Y. Wu, C. Yi, G.-Y. Qin, and S. Pu, *Phys. Rev. C* **105** (2022) 064909.
17. R. L. S. Farias, W. R. Tavares, R. M. Nunes, and S. S. Avancini, *Eur. Phys. J. C* **82** (2022) 674.
18. H. T. Ding, S. T. Li, Q. Shi, A. Tomiya, X. D. Wang, and Y. Zhang, *Acta Phys. Polon. Supp.* **14** (2021) 403.
19. H. T. Ding, S. T. Li, Q. Shi, and X. D. Wang, *Eur. Phys. J. A* **57** (2021) 202.
20. R. K. Mohapatra, *Phys. Rev. C* **99** (2019) 024902.
21. M. D'Elia, L. Maio, F. Sanfilippo, and A. Stanzione, *Phys. Rev. D* **104** (2021) 114512.
22. R. Ghosh and N. Haque, *Phys. Rev. D* **105** (2022) 114029.
23. C. Grayson, M. Formanek, J. Rafelski, and B. Müller, *Phys. Rev. D* **106** (2022) 014011.
24. K. K. Gowthama, M. Kurian, and V. Chandra, *Phys. Rev. D* **106** (2022) 034008.
25. K. Hattori, M. Hongo, and X.-G. Huang, *Symmetry* **14** (2022), `https://doi.org/10.3390/sym14091851`.
26. D. Teng and X. Guo, *Chin. Phys. C* **46** (2022) 094104.
27. G. S. Bali *et al.*, *JHEP* **02** (2012) 044.
28. G. S. Bali, F. Bruckmann, G. Endrodi, Z. Fodor, S. D. Katz, and A. Schafer, *Phys. Rev. D* **86** (2012) 071502.
29. G. S. Bali, F. Bruckmann, G. Endrodi, F. Gruber, and A. Schaefer, *JHEP* **04** (2013) 130.
30. G. S. Bali, F. Bruckmann, G. Endrödi, S. D. Katz, and A. Schäfer, *JHEP* **08** (2014) 177.
31. R. A. Schneider and W. Weise, *Phys. Rev. C* **64** (2001) 055201.
32. J.-P. Blaizot, E. S. Fraga, and L. F. Palhares, *Phys. Lett. B* **722** (2013) 167.
33. A. Ayala, C. A. Dominguez, L. A. Hernandez, M. Loewe, and R. Zamora, *Phys. Rev. D* **92** (2015) 096011. [*Phys. Rev. D* **92** (2015) 119905].

34. S. Rath and B. K. Patra, *JHEP* **12** (2017) 098.
35. B. Karmakar, R. Ghosh, A. Bandyopadhyay, N. Haque, and M. G. Mustafa, *Phys. Rev. D* **99** (2019) 094002.
36. D. E. Kharzeev, K. Landsteiner, A. Schmitt, and H.-U. Yee, *Lect. Notes Phys.* **871** (2013) 1.
37. I. A. Shovkovy, *Particles* **5** (2022) 442.
38. B. Karmakar, R. Ghosh, A. Bandyopadhyay, N. Haque, and M. G. Mustafa, *Springer Proc. Phys.* **277** (2022) 359.
39. S. K. Das *et al.*, *Int. J. Mod. Phys. E* **31** (2022) 12.
40. E. S. Fraga, L. F. Palhares, and T. E. Restrepo, (2023).
41. D. H. Rischke, *Progress in Particle and Nuclear Physics* **52** (2004) 197.
42. S. K. Ghosh, T. K. Mukherjee, M. G. Mustafa, and R. Ray, *Phys. Rev. D* **73** (2006) 114007.
43. M. Bluhm, B. Kämpfer, and G. Soff, *Physics Letters B* **620** (2005) 131.
44. A. Ayala, M. Loewe, J. C. Rojas, and C. Villavicencio, *Phys. Rev. D* **86** (2012) 076006.
45. Y. B. Ivanov, V. V. Skokov, and V. D. Toneev, *Phys. Rev. D* **71** (2005) 014005.
46. S. Koothottil and V. M. Bannur, *Phys. Rev. C* **99** (2019) 035210.
47. L.-J. Luo, J. Cao, Y. Yan, W.-M. Sun, and H.-S. Zong, *Eur. Phys. J. C* **73** (2013) 2626.
48. V. M. Bannur, *Int. J. Mod. Phys. A* **29** (2014) 1450056.
49. P. F. Valenzuela-Coronado, Propiedades termodinámicas del plasma de quarks-gluones usando un modelo de cuasipartícula, Master's thesis, División de Ciencias e Ingenierías, Universidad de Guanajuato (2020), `https://www.repositorio.ugto.mx/`.
50. M. I. Gorenstein and S. N. Yang, *Phys. Rev. D* **52** (1995) 5206.
51. S. Koothottil and V. M. Bannur, *Phys. Rev. C* **99** (2019) 035210.
52. R. L. S. Farias, K. P. Gomes, G. Krein, and M. B. Pinto, *Phys. Rev. C* **90** (2014) 025203.
53. J. O. Andersen, W. R. Naylor, and A. Tranberg, *Rev. Mod. Phys.* **88** (2016) 025001.
54. N. Mueller and J. M. Pawlowski, *Phys. Rev. D* **91** (2015) 116010.
55. M. D'Elia, F. Manigrasso, F. Negro, and F. Sanfilippo, *Phys. Rev. D* **98** (2018) 054509.
56. A. Ayala, M. Loewe, and R. Zamora, *Phys. Rev. D* **91**, (2015) 016002.
57. M. Kurian, *Phys. Rev. D* **102** (2020) 014041.
58. M. Thaler, *Technische Univ. Muenchen, Garching* (Germany) (2006), `https://d-nb.info/978932617/34`.
59. C. Ratti, M. A. Thaler, and W. Weise, *Phys. Rev. D* **73** (2006) 014019.
60. A. Ayala *et al.*, *Phys. Rev. D* **94** (2016) 054019.